

## Plasticity of Ductile Metallic Glasses: A Self-Organized Critical State

B. A. Sun, H. B. Yu, W. Jiao, H. Y. Bai, D. Q. Zhao, and W. H. Wang\*

*Institute of Physics, Chinese Academy of Sciences, Beijing 100190, China*

(Received 21 March 2010; published 13 July 2010)

We report a close correlation between the dynamic behavior of serrated flow and the plasticity in metallic glasses (MGs) and show that the plastic deformation of ductile MGs can evolve into a self-organized critical state characterized by the power-law distribution of shear avalanches. A stick-slip model considering the interaction of multiple shear bands is presented to reveal complex scale-free intermittent shear-band motions in ductile MGs and quantitatively reproduce the experimental observations. Our studies have implications for understanding the precise plastic deformation mechanism of MGs.

DOI: 10.1103/PhysRevLett.105.035501

PACS numbers: 62.20.F–

Understanding the plastic flow of materials in the context of nonequilibrium statistic mechanics has received considerable interest [1,2]. For crystalline solids, their plastic deformation is a complex inhomogeneous process, and the dislocation motions are characterized by scale-free and intermittent avalanches [3,4], which are reminiscent of the concept of self-organized criticality (SOC) [5]. Metallic glasses (MGs) have a disordered atomic microstructure which is completely different from that of crystalline materials. The plastic deformation of MGs at room temperature is accomplished via highly localized nanoscale shear bands [6,7], which manifest as serrated flow behavior in stress-strain curves. The plasticity of MG relates to some properties [8,9] or testing conditions [10], and useful criteria were proposed to predict the ductility of MGs, while the plasticity of MGs is an intrinsically dynamical phenomenon and should be closely related to the dynamical features. Extensive investigations have shown that MGs exhibit a ubiquitous serrated flow behavior with dynamic characteristics in the plastic deformation regime [11–14]. In this Letter, we find that the macroscopic plasticity of MGs correlates closely with the dynamical behavior of serrated flows. A stick-slip model considering the interaction of multiple shear bands is constructed for quantitatively reproducing the basic experimental observations.

The homologous cylindrical MG rods (2 mm in diameter) were prepared by arc melting and copper mold casting [15]. Compressive cylindrical specimens were cut out of the as-cast rods with an aspect ratio of 2:1. Mechanical tests were carried out at room temperature in an Instron electromechanical 3384 test system. The parameters were measured and digitally stored at a frequency of 50 Hz. Figure 1(a) shows stress-strain curves of eight typical MGs. All the curves exhibit serrated flow behaviors characterized by repeated cycles of a sudden stress drop [highlighted in Fig. 1(b)] followed by reloading elastically. Their mechanical properties are summarized in Table I. These MGs can be divided into two distinct groups according to their plasticity. The first group (the first four alloys in Table I) shows limited plasticity ( $\epsilon_p < 5\%$ ), and the latter four MGs with large plasticity ( $\epsilon_p > 10\%$ ) com-

pose the second group. Figure 1(c) contrasts the segments of stress-strain curves at the same strain range for typical brittle  $Zr_{52.5}Ti_5Cu_{17.9}Ni_{14.6}Al_{10}$  (Vit105) and ductile  $Cu_{47.5}Zr_{47.5}Al_5$ . The serrations for the ductile MGs display various sizes, which are more complex than those in the first group. To quantify this, we measured the amplitude of stress drop associated with each serration and analyzed its statistical properties for individual deformation curves in the plastic regime. Before the statistics, a normalization of stress drop magnitude is deemed necessary as the strain causes a systematic “shift” of the statistics. Using a linear regression fit through a stress drop size vs strain diagram,  $\overline{\Delta\sigma_s} = f(\epsilon)$ , the distribution of the normalized stress drops,  $s = \Delta\sigma_s/f(\epsilon)$ , was considered. We note that some tiny stress undulations induced by the vibration of the cross head of testing machine appear on the serrations events and

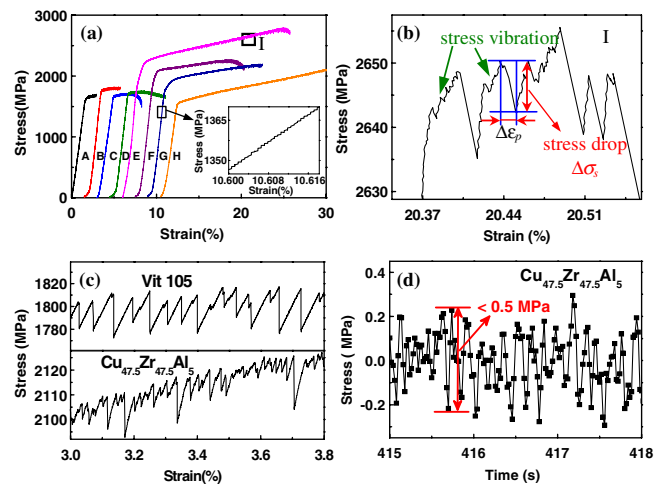


FIG. 1 (color online). (a) Strain-stress curves (strain rate =  $1 \times 10^{-4}$ /s) of typical MGs listed in Table I. The inset is an enlarged elastic part showing the stress vibrations due to the testing machine. (b) Enlarged serrations in region I, showing the stress drop of a serration. (c) Comparison of the serrated flows of Vit105 and  $Cu_{47.5}Zr_{47.5}Al_5$  MGs at the same strain range. (d) An example of stress vibrations due to the testing machine by subtracting the linear fitting from the stress-time curve in the elastic range for  $Cu_{47.5}Zr_{47.5}Al_5$ .

TABLE I. The yielding stress  $\sigma_y$ , plastic strain  $\varepsilon_p$  for the MGs imposed to strain rate  $1 \times 10^{-4}$ , their dynamics of serrated flow, and the power-law exponent  $\alpha$ .

MG label	MG	$\sigma_y$ (MPa)	$\varepsilon_p$ (%)	$\alpha$	Dynamics of serrated flow
A	Zr <sub>41.25</sub> Ti <sub>13.75</sub> Ni <sub>10</sub> Cu <sub>12.5</sub> Be <sub>22.5</sub> (Vit1)	1600	1.50	...	Chaos
B	Zr <sub>52.5</sub> Ti <sub>5</sub> Cu <sub>17.9</sub> Ni <sub>14.6</sub> Al <sub>10</sub> (Vit105)	1740	2.26	...	Chaos
C	Zr <sub>57</sub> Nb <sub>5</sub> Cu <sub>15.4</sub> Ni <sub>12.6</sub> Al <sub>10</sub> (Vit106)	1650	3.32	...	Chaos
D	Zr <sub>61.2</sub> Cu <sub>15.75</sub> Ni <sub>13.05</sub> Al <sub>10</sub>	1703	4.56	...	Chaos
E	Vit105 (pretreated [16])	1980	18	1.41	SOC
F	Cu <sub>47.5</sub> Zr <sub>47.5</sub> Al <sub>5</sub>	1810	10.9	1.49	SOC
G	Zr <sub>62</sub> Cu <sub>15.5</sub> Ni <sub>12.5</sub> Al <sub>10</sub>	1765	11.5	1.48	SOC
H	Zr <sub>64.13</sub> Cu <sub>15.75</sub> Ni <sub>10.12</sub> Al <sub>10</sub>	1532	>30	1.37	SOC

the elastic deformation range [17] [insets in Figs. 1(a) and 1(b)]. By subtracting the linear fitting part from the elastic deformation range [see Fig. 1(d)], the stress vibrations are no more than 0.5 MPa. Thus, the serrations with  $\Delta\sigma_s < 0.5$  MPa are not counted in our statistics.

The distribution histograms of stress drops for two typical MGs are shown in Fig. 2. One can see that the distribution closely correlates with the plasticity. For Vit105, the distribution histograms display a peak shape which is similar to a chaotic dynamics of jerk flow in single crystals [18]. The time series analysis to the deformation curves for the MGs in the first group by calculating the correlation dimension and the Lyapunov spectrum indeed confirm the chaotic dynamics for these alloys [19]. The dominant deformation mode of these brittle MGs is a primary single shear band along the principal shear plane, and few secondary shear bands can be observed. The relation between the serrated flows and the single shear band moving in the brittle MGs has been extensively studied [10,13,17], and a stick-slip model can give the relation between the shear step size of single shear band and the load drop [20], while in plastic MGs the load often induces simultaneous formation and interaction of multiple shear bands [21]. The serrations of the ductile MGs such as Cu<sub>47.5</sub>Zr<sub>47.5</sub>Al<sub>5</sub> are more complex and display a monotonically decreasing distribution in sharp contrast with that of brittle MGs such as Vit105 (Fig. 2). We then focus on the dynamics of those complex ductile MGs in this work. To quantify the statistical data, the distribution density  $D(s) = (1/N) \times [\delta N(s)/\delta s]$  was calculated. Here  $\delta N(s)$  is the number of stress drops whose normalized magnitude falls into the interval  $(s - \delta s/2, s + \delta s/2)$ , and  $N$  is the total number of drops. For large  $s$ , a variable width of the interval  $\delta s$  was used as the number of data points becomes progressively small. The calculated  $D(s)$  for Cu<sub>47.5</sub>Zr<sub>47.5</sub>Al<sub>5</sub> can be well described by a power-law distribution  $D(s) \sim s^{-\alpha}$  with an exponent  $\alpha = 1.49$ , as shown in Fig. 3. The slight scatter of the data points at larger  $s$  may arise from the finite-size effect [5]. Similar behavior is also found in other ductile MGs with the calculated  $\alpha$  in the range of 1.3–1.5 (see Table I).

Previous studies [11–14,20] have shown that the stress drop in serrated flow of MGs arises from the rapid sliding

of shear bands, and its amplitude can be used as a measure of the size of plastic event or avalanche during the deformation. The shear displacement rate during the plastic event is measured to be  $\sim 10^{-4}$  ms<sup>-1</sup> [11], which is 2 orders larger than our loading rate ( $4 \times 10^{-7}$  ms<sup>-1</sup>), suggesting that the stress loading process, which is much lower than the internal relaxation process, is an external slow driving force. In addition, the large plasticity of MGs indicates the formation and interaction of multiple shear bands during plastic deformation [21]. The power-law distribution of plastic avalanches and a large number of interacting entities (shear bands) as well as the external slow driving forces suggest that the plastic deformation of ductile MGs should be considered in the framework of the SOC [22]. We emphasize that the emergence of SOC is closely related to the ductility of MGs. When the ductility of Vit105 was improved by pretreatment [16], its dynamics of serrated flow also changed from chaos to SOC (see Table I). The SOC, which has been observed in many complex systems in various fields [22], means that the

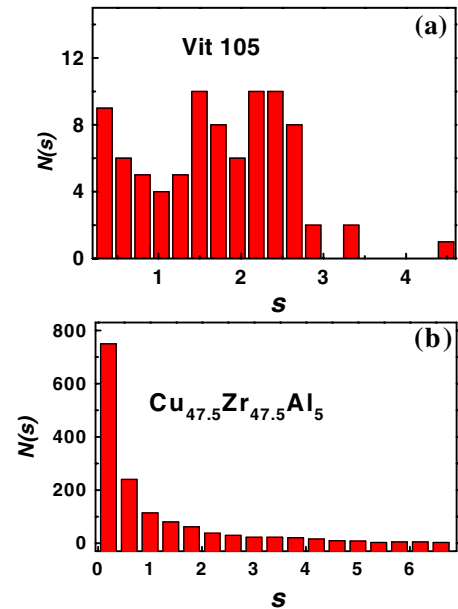


FIG. 2 (color online). (a) Number of stress drops  $N(s)$  vs the normalized stress drop magnitude  $s$  for (a) Vit105 and (b) Cu<sub>47.5</sub>Zr<sub>47.5</sub>Al<sub>5</sub> MGs.

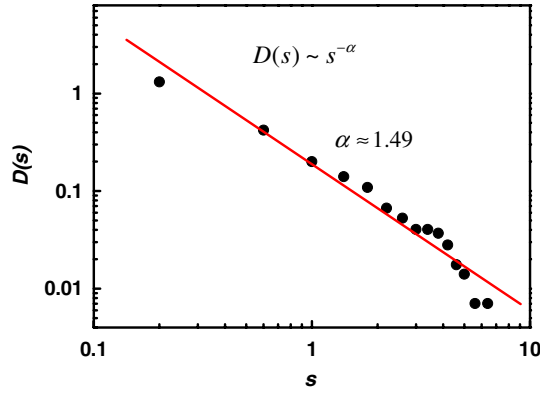


FIG. 3 (color online). Log-log plot of the density distribution  $D(s)$  vs normalized stress drop magnitude  $s$  for  $\text{Cu}_{47.5}\text{Zr}_{47.5}\text{Al}_5$ , which can be fitted by a power-law scaling with  $\alpha = 1.49$ .

system can buffer against large changes, although not completely immune to them, and endure intervention as any external impact on such a complex system is dissipated throughout the networks of connected participants. Thus, SOC dynamics can result in a large stable plastic range for ductile MGs. The result may have implication for exploring MGs with large plasticity.

The emergence of the SOC state indicates that one must consider the effect of shear-band interaction on the dynamics behavior during the deformation of ductile MGs. The stick-slip model [20] for single dominant shear band during the deformation of MGs considered a closed system consisting of a MG sample and an elastic spring representing the influence of testing machine, which provides a basic picture of single shear-band instability process of MGs. Here we extended the model to multiple shear bands by considering their interactions. Directly calculating the interaction of multiple shear bands is extremely complex as every shear-band sliding causes the stress redistribution and affects other operating shear bands. We consider a system consisting of  $N$  blocks of equal effective mass  $M$ , as illustrated in Fig. 4. Each block is loaded independently by an elastic spring with strength  $k$  at a slowly constant rate  $v$  and connects to its two neighbors by springs of strength  $k_c$ . Thus, the shear-band sliding of one block only has elastic interaction to its two neighbors via the connecting springs, and the kinetic equation is

$$[k(vt - x_i) + k_c(x_{i+1} + x_{i-1} - 2x_i) - \sigma_f(\dot{x}_i)] \frac{\pi d^2}{4} = M\ddot{x}_i, \quad (1)$$

where  $d$  is the sample diameter,  $x_i$  is the shear sliding displacement of the  $i$ th block, and  $\dot{x}_i$  and  $\ddot{x}_i$  are its first and second derivatives, respectively. By a comparison with the kinetic equation in Ref. [20], we obtained  $k = E/L(1 + S)$ , where  $L$  is the sample height,  $E$  is the Young's modulus, and  $S$  is the stiffness ratio of sample to the testing machine.  $\sigma_f$  is the shear resistance along the shear plane. When the driving forces exceed the static

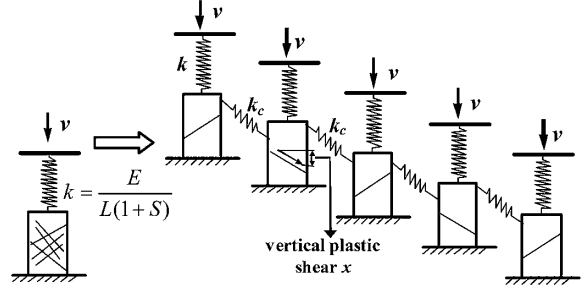


FIG. 4. Schematic diagram of the stick-slip model incorporating the interaction of multiple shear bands for ductile MGs.

shear resistance for one block, shear sliding will occur corresponding to the formation of one shear band.  $\sigma_f$  is a complex function of the strain rate and temperature in the shear band [20]. As the temperature rise is also dependent on strain rate, we assume  $\sigma_f$  is only a function of  $\dot{x}_i$  and in the simple form  $\sigma_f = \sigma_{f0}/(1 + A\dot{x}_i)$ , with  $\sigma_{f0}$  taken as the yielding strength of sample and  $A$  being a constant. For typical Zr-based MGs, we choose  $A = 5$ , meaning that when the sliding speed  $\dot{x}_i$  is 0.002 m/s, the drop of  $\sigma_f$  is  $\sim 20$  MPa and the calculated temperature rise  $\Delta T$  [ $\sigma_f(T) = \sigma_f(T_R) - AE\Delta T/T_g$  [23]] is about 15 K consistent with the results in Ref. [20]. Although the form of  $\sigma_f(\dot{x}_i)$  is taken a little arbitrarily, we will show below that the key point is the negative strain rate sensitivity of  $\sigma_f$ , not its form, playing the dominant role in the dynamics of shear bands.

Equation (1) has a uniform solution in which all shear bands slide at the loading rate  $v$ :  $x_i = vt - \frac{1}{k}\sigma_f(v)$ . This solution is unstable to both uniform and spatially varying perturbations in  $x$ . A straightforward linear stable analysis suggests that all Fourier modes grow exponentially, and the sufficient condition for the instability is  $d\sigma_f/d\dot{x}|_{\dot{x}=v} < 0$ . Equation (1) also has periodic solutions in which the system alternatively sticks and slides, as if it were a single block when the initial conditions are spatial homogenous. The solution is unstable to spatial variations also due to  $d\sigma_f/d\dot{x} < 0$ . We then solved Eq. (1) numerically for various values of  $k_c$  ( $k_c = 0.1k, 0.25k, 0.5k$ , and  $0.8k$ ) and system size up to  $N = 200$ . The values of materials parameters are chosen for the typical Zr-based MGs [24]. Generally, we start the system at  $t = 0$  with small spatial inhomogeneity and used the period boundary conditions. After elastically deformed for a period  $\tau_e = \sigma_{f0}/kv$ , the system entered into the plastic deformation regime in which we observed a wide range of events corresponding to the rapid shear-band motions. Some events are illustrated in Fig. 5(a) in the form of graphs of  $\dot{x}_i$  as a function of positions  $i$  and  $t$ . Except for small events involving only one sliding of a block, large events in which several blocks participated can also be observed, indicating cooperative shear-band sliding. And these sliding events appeared in an intermittent, trigger-aftershock pattern in which small events lead to smoothing in a larger scale, resulting in

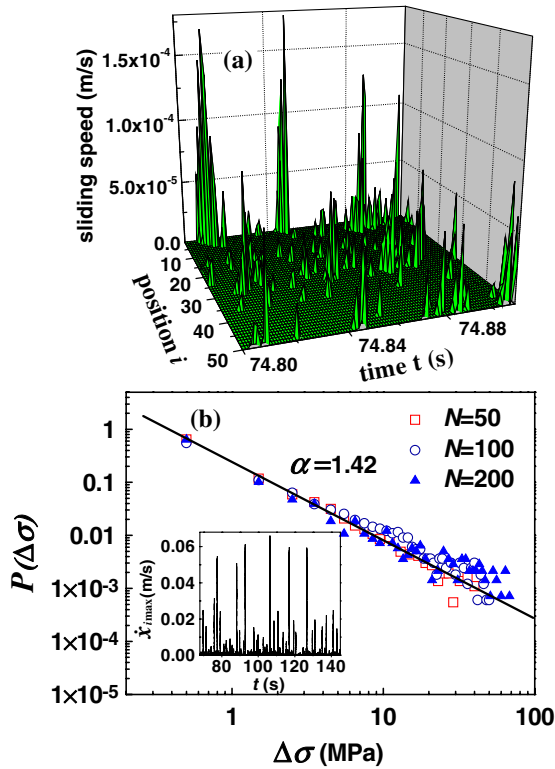


FIG. 5 (color online). Numerical solutions for the stick-slip model of multiple shear bands. (a) Sliding speed  $\dot{x}_i$  vs the position  $i$  and time  $t$  for  $N = 50$  and  $k_c = 0.8k$ , showing sliding events of various sizes. (b) The probability distributions  $P(\Delta\sigma)$  of stress drops for different system size at  $k_c = 0.8k$ , well fitted by a power law  $P(\Delta\sigma) \sim \Delta\sigma^{-\alpha}$ . The inset shows the maximum sliding speed  $\dot{x}_{i\max}$  with  $t$  for  $N = 200$ . The parameters used are  $E = 90$  GPa,  $\sigma_{f0} = 2.0$  GPa,  $M = 20$  Kg,  $v = 4.0 \times 10^{-6}$  m/s, and  $S \approx 2$  (Ref. [20]) for  $d = 2$  mm,  $L = 4$  mm.

larger events later on, similar to what happened in the fault dynamics [25].

For a deformed MG with multiple shear bands, its instantaneous displacement of the sample head is determined by the shear band with the fastest sliding rate, so the stress drop due to the sliding event in our model can be calculated by  $\Delta\sigma = k \int_{\text{event}} (\dot{x}_{i\max} - v) dt$ , where  $\dot{x}_{i\max}$  is the maximum sliding rate among the blocks involved in the sliding events at  $t$ . The statistics of  $\Delta\sigma$  for our numerical results can be well described by a power-law distribution for different system sizes, as exemplified in Fig. 5(b) at  $k_c = 0.8k$  with the fitting exponent  $\alpha = 1.42$ , which falls into the experimental range of 1.3–1.5, suggesting our model captures the basic features of plastic deformation of ductile MGs. Other  $k_c$  yield similar results except for the weak  $k_c = 0.1k$ , which deviates from the power-law distribution, confirming the interaction of shear bands is the governing factor in their dynamics. Similar numerical solutions are also obtained in other ductile MGs. The power distribution of  $\Delta\sigma$  reveals that the shear-band motions in ductile MGs are in a complex, scale-free intermittent fashion and verifies the SOC behavior of our

observations. Our model has a very similar form with that of fault dynamics [25], and the plastic deformation of ductile MGs could be used as a laboratory system to mimic earthquakes.

In summary, we demonstrate by both experimental studies and theoretical analysis that the plastic deformation of ductile MGs can evolve into a self-organized critical state characterized by intermittent power-law distributed shear avalanches. Our studies suggest that the shear-band interactions should be considered in understanding of the dynamics behavior of deformation in ductile MGs.

The financial support is from the NSF of China (No. 50731008 and No. 50921091) and MOST 973 (No. 2007CB613904 and No. 2010CB731603).

\*Corresponding author.

whw@aphy.iphy.ac.cn

- [1] G. Nsar and W. Daniel, *Instabilities and Self-Organization in Materials* (Oxford Scholarship Online, 2008).
- [2] P. Sammonds, *Nature Mater.* **4**, 425 (2005).
- [3] M. C. Miguel *et al.*, *Nature (London)* **410**, 667 (2001); M. Koslowski, R. Lesar, and R. Thomson, *Phys. Rev. Lett.* **93**, 125502 (2004).
- [4] J. Weiss and D. Marsan, *Science* **299**, 89 (2003).
- [5] P. Bak, C. Tang, and K. Wiesenfeld, *Phys. Rev. A* **38**, 364 (1988).
- [6] F. Spaepen, *Acta Metall.* **25**, 407 (1977); A. S. Argon, *Acta Metall.* **27**, 47 (1979).
- [7] M. L. Falk and J. S. Langer, *Phys. Rev. E* **57**, 7192 (1998).
- [8] J. Schroers and W. L. Johnson, *Phys. Rev. Lett.* **93**, 255506 (2004).
- [9] J. J. Lewandowski, W. H. Wang, and A. L. Greer, *Philos. Mag. Lett.* **85**, 77 (2005).
- [10] Z. Han *et al.*, *Acta Mater.* **57**, 1367 (2009).
- [11] W. J. Wright, R. Saha, and W. D. Nix, *Mater. Trans.* **42**, 642 (2001).
- [12] F. H. D. Torre *et al.*, *Appl. Phys. Lett.* **89**, 091918 (2006).
- [13] C. A. Schuh and T. G. Nieh, *Acta Mater.* **51**, 87 (2003).
- [14] A. L. Greer *et al.*, *Mater. Sci. Eng. A* **375–377**, 1182 (2004).
- [15] W. H. Wang, *Prog. Mater. Sci.* **52**, 540 (2007).
- [16] H. B. Yu *et al.*, *Scr. Mater.* **61**, 640 (2009).
- [17] G. Wang *et al.*, *Acta Mater.* **57**, 6146 (2009); S. X. Song and T. G. Nieh, *Intermetallics* **17**, 762 (2009).
- [18] G. Ananthakrishna *et al.*, *Phys. Rev. E* **60**, 5455 (1999).
- [19] G. Ananthakrishna and B. A. Sun (unpublished).
- [20] Y. Q. Cheng, Z. Han, Y. Li, and E. Ma, *Phys. Rev. B* **80**, 134115 (2009).
- [21] J. Das *et al.*, *Phys. Rev. Lett.* **94**, 205501 (2005); Y. H. Liu *et al.*, *Science* **315**, 1385 (2007).
- [22] H. J. Jensen, *Self-Organized Criticality* (Cambridge University Press, Cambridge, England, 1998).
- [23] H. Li, C. Fan, H. Choo, and P. K. Liaw, *Mater. Trans., JIM* **48**, 175 (2007).
- [24] G. He, W. Löser, J. Eckert, and L. Schultz, *Acta Mater.* **51**, 2383 (2003).
- [25] J. M. Carlson and J. S. Langer, *Phys. Rev. Lett.* **62**, 2632 (1989).